AJBMS AFGHANISTAN Journal of Basic Medical Sciences
ISSN: 3005-6632

Afghanistan Journal of Basic Medical Sciences

2026 Jan; 3(1): 53-74.

ajbms.knu.edu.af

Mechanistic Insights from Docking and Dynamics: Soy Isoflavonoids Disrupt *Pseudomonas aeruginosa* Quorum Sensing by Targeting AHL Synthase LasI

Abdullah Ahmadzai[1], Fahim Amirkhezi[1,] *Abdul Musawer Bayan[1], Muhammad Qadar Adel[2], Abdullah Sahar[3], Mohammad Reza Mowahhed[1], Ehsanullah Rasoly[1], Rafiullah Shirzadi[1], Mohammad Ehsanullah Noorkhail[1]

1. *Medical Sciences Research Center, Ghalib University, Kabul, Afghanistan*
2. *Department of Internal Medicine, Faculty of Medicine, Spinghar University, Kabul, Afghanistan*
3. *Department of Microbiology, Faculty of Medical Laboratory Technology, Spinghar University, Kabul, Afghanistan*

ARTICLE INFO

Type: Original Article

Received: 11 Oct, 2025

Accepted: 28 Dec, 2025

*Corresponding Author:
E-mails: abdulmusawerbayan@gmail.com

To cite this article:

Ahmadzai A, Amirkhezi F, Bayan AM, Adel MQ, Sahar A, Mowahhed MR, Rasoly E, Shir-zadi R, Noorkhail ME. Mechanistic Insights from Docking and Dynamics: Soy Isoflavonoids Disrupt P. Aeruginosa Quorum Sensing by Targeting AHL Synthase LasI. Afghanistan Journal of Basic Medical Sciences. 2026 Jan; 3(1): 53-74.

DOI:
https://doi.org/10.62134/khatamuni.145

ABSTRACT

Background: The increasing prevalence of multidrug-resistant necessitates alternative therapeutic strategies that attenuate virulence rather than inhibit bacterial growth. Quorum sensing (QS) is a central regulator of virulence and biofilm formation in this pathogen, with the acyl-homoserine lactone synthase LasI functioning as a master regulator within the QS hierarchy. Natural products such as soy isoflavonoids represent promising anti-virulence candidates; however, their mechanistic interactions with LasI remain insufficiently characterized.

Methods: An integrated *in silico* approach was applied to investigate the inhibitory potential of genistein, daidzein, and glycitein against LasI synthase. Molecular docking using AutoDock 4.2.2 was conducted to predict binding modes and affinities, followed by molecular dynamics simulations with GROMACS 2019.6 to evaluate structural stability and conformational dynamics.

Results: All three isoflavonoids exhibited stable binding within the LasI active site, involving conserved interactions with key residues Arg30 and Val143. Molecular dynamics analyses revealed distinct mechanistic effects: genistein markedly stabilized the enzyme structure, glycitein induced rapid equilibration and global compaction, while daidzein increased conformational flexibility, suggesting a possible allosteric mode of inhibition. MM/PBSA calculations identified genistein as the most energetically favorable ligand, predominantly driven by van der Waals interactions.

Conclusion: Soy isoflavonoids inhibit LasI synthase through distinct structural mechanisms, with genistein emerging as a promising scaffold for anti-quorum sensing drug development. This strategy offers a potential narrow-spectrum approach to mitigating *P. aeruginosa* virulence with reduced selective pressure for resistance.

Keywords: *Pseudomonas aeruginosa*, Quorum sensing, LasI AHL synthase, *In Silico*, Soy Isoflavonoids

Introduction

The growing crisis of antimicrobial resistance (AMR) is one of the greatest challenges facing public health in the 21st century (1). This problem is exemplified by opportunistic pathogens such as *Pseudomonas aeruginosa*, a Gram-negative bacterium infamous for producing severe, frequently untreatable, infection in the immunocompromised host, burn patients, and individuals with cystic fibrosis (2-4). The stubbornness of *P. aeruginosa* infection is not solely the result of intrinsic resistance to a broad class of drugs but deeply magnified by its capability for forming tough, surface-connected communities of bacteria referred to as biofilms (5, 6).

A biofilm consists of a structured community of bacterial cells embedded in a self-secreted matrix of extracellular polymeric substances (EPS), comprising polysaccharides, proteins, and extracellular DNA (7). As a result, biofilm-based infections are extremely resistant to eradication, with attendant high levels of morbidity, mortality, and health care costs (8, 9). The inability of traditional antibiotics to adequately access and eliminate biofilm communities has generated a compelling need for therapeutic modalities operating by a mode other than the traditional bactericidal one (9-11). Quorum sensing (QS) enables the bacterial population to detect the local cell density and change gene expression coordinately as a population (12). This process occurs via the production, release, and perception of small diffusible signals, the autoinducers (13). As the population grows, the level of the autoinducers builds up in the environment (14). *P. aeruginosa* relies upon a hierarchically structured QS network centered mainly on two acyl-homoserine lactone (AHL) signaling systems, the Las and the Rhl systems (15). AHLs represent the prototypical QS signals for Gram-negative bacteria (16). The AHL diffuses freely through the membranes of the bacteria and when reaching the critical concentration binds with the cognate transcriptional regulator LasR (17). This holds the hope of a more sustainable therapeutic strategy. Third, such a strategy forms the very essence of a narrow-spectrum approach, mainly impacting those pathogens utilizing AHL-based QS, such as *P. aeruginosa*, thus saving the benign host microbiome from the usual side effects of broad-spectrum antibiotics (18). As a potential lead for effective synthase lasI inhibitors, natural products provide a wealth of pre-existing, biologically validated sources of chemical scaffolds (18).

Soybean isoflavonoids, including genistein, daidzein, and glycitein, come into strong focus as promising lead molecules (19). These natural compounds are not only highly abundant and safe for human consumption but also possess a wide spectrum of documented medical benefits (20). The primary soybean isoflavones such as genistein, daidzein, and glycitein have been extensively studied for their therapeutic potential (21). Genistein is renowned for its potent antioxidant (22), anticancer (23), and phytoestrogenic activities (24). It has been investigated for its role in mitigating menopausal symptoms (25), preventing osteoporosis by modulating bone metabolism (26), and inhibiting the proliferation of various cancer cells (27, 28), particularly in breast and prostate cancer. Daidzein shares similar benefits, including cardioprotective effects through the improvement of lipid profiles and vascular function (29, 30). It is notably metabolized by gut microbiota to equol, a compound with even stronger estrogenic and antioxidant activities (29, 31). Glycitein, while less studied, also exhibits estrogenic properties and has shown neuroprotective and antidiabetic potential in preclinical models (32-36). Crucially, nascent evidence also suggests intrinsic against a variety of pathogens (37-39).

Yet, against these promising associations, a vital gap persists: the exact, atomistic mechanism

by which these isoflavonoids interact and inhibit the synthase LasI enzyme remains completely unstudied. Determining whether they operate as competitive inhibitors, allosteric modulators, or broader structural destabilization is cardinal for their rational development into effective and selective therapeutic agents.

To close this gap, we utilized a computational technique such as molecular docking and molecular dynamic simulation for the study of molecular interaction between the synthase LasI and the soy isoflavonoids.

Materials and Methods

Protein and Ligand structure selection

The structure of *P. aeruginosa* acyl-homoserine lactones synthase LasI with PDB code 1RO5, downloaded from RCSB protein data bank (40). And the 3D structure of Genistein, Daidzein, and Glycitein with CID (5280961, 5281708, 5317750) codes was obtained from PubChem database in SDF format and converted to PDB format using Open Babel software respectively (41).

Molecular docking

To Interrogate the interactions and binding affinity between genistein, daidzein, or glycitein and synthase LasI (1RO5), we employed a docking technique using Autodock 4.2.2 (42). Proteins structures initially prepared for docking by removing water molecules and co-crystal ligands existed in pdb files and hydrogen atoms with Gasteiger charges added to the system. Subsequently, before proceeding docking method, energy minimization of proteins preformed utilizing GROMACS 2019.6 package using AMBER99SB force field (43). The active sites of proteins were determined by co-crystal ligand reported in pdb file of proteins and then the grid box with the dimensions of 60×60×60 points and a grid point spacing of 0.375 Å was selected. Eventually, 200 docking calculations consisted of the 25 million energy evaluations by using Lamarckian genetic algorithm (LGA) method were performed. Finally, the lowest binding energy conformation in the maximum populated cluster was chosen as the best docking pose and used for molecular dynamic simulation input files.

Molecular dynamic simulation

Investigation of complexes between genistein, daidzein, or glycitein and 1RO5 carried out applying MD simulation technique with more details. MD simulation performed for the three proteins in the free form and in complex with genistein, daidzein, and glycitein in a cubic box solvated by water tip3p model, by GROMACS 2019.6 program using the AMBER99SB force field executed on Kubuntu 2020.4 LINUX operating system, parameters for genistein, daidzein, or glycitein were generated using the Pythonbased ACPYPE tool (AnteChamber Python Parser Interface) (44). Enough number of Na+ or Cl- ions were added to neutralize system charges and achieve to the physiological ion concentration of 0.15 M. In the first step rapid descend method utilized for energy minimization process. Then energy minimized systems were balanced with 1ns simulations in nvt and not ensembles in 310 K and 1 bar. After the systems were well balanced, MD run was performed with a time step of 2 fs for 200 ns simulation time. Eventually, simulated trajectories were used to study the molecular structure of protein, ligand and intermolecular interactions during the simulation time. For analysis purposes, plots for root mean square deviation (RMSD), root mean square fluctuation (RMSF), radius of gyration (Rg), and solvent accessible surface area (SASA), along with hydrogen bond analysis, were generated and analysed.

Results

Molecular docking

Molecular docking analysis demonstrated that the isoflavonoids genistein, daidzein, and glycitein exhibit strong binding affinity for the synthase LasI, with daidzein showing the most potent inhibition potential (ΔG = -7.90 kcal/mol; Ki = 1.62 µM), closely followed by glycitein (ΔG = -7.82 kcal/mol; Ki= 1.85 µM) and genistein (ΔG = -7.51 kcal/mol; Ki = 3.13 µM), as shown in Table 1. The high number of conformations in the top-ranked clusters (Genistein: 198; Daidzein: 200; Glycitein: 128) indicates a stable and reliable binding pose for each complex. The all complexes (Fig. 1a, 1b and 1c) revealed a multifaceted interaction network involving key residues Arg30 and Val143. The ligands are stabilized within the binding pocket through hydrogen bonds interactions with Arg30 and Val143.

In the Synthase LasI/Genistein complex (Fig. 1a), distinct binding patterns emerged with hydrogen bonds between: Genistein's carbonyl group and Arg30 (2.64 Å); and its hydroxyl group with Val143 (2.76 Å). These variations highlight Genistein's structural flexibility in accommodating different enzyme microenvironments. Similarly, the Synthase LasI/Daidzein complex (Fig. 1b), also shows hydrogen bonds interactions between: Daidzein's carbonyl group and Arg30 (2.64 Å); and its hydroxyl group with Val143 (2.76 Å). The Synthase LasI/Glycitein (Fig. 1c), also follow the above interaction hydrogen bonds pattern, in which the glycitein maintained a hydrogen bond with carbonyl group of Arg30 (2.63 Å) and hydroxyl group of Val143 (2.68 Å). Comparative analysis of the three complexes reveals a conserved interaction with a critical cluster of residues, including Arg30 and Val143. This suggests a shared binding region and a common inhibition mechanism despite the subtle structural differences between the isoflavonoids. The variations in the precise interaction networks explain the differences in their binding energies and inhibitory constants.

These findings collectively suggest that isoflavonoids, particularly daidzein and glycitein, possess significant potential as inhibitors of synthase LasI. The conserved interactions with key hydrophobic and polar residues provide a robust structural foundation for developing optimized synthase LasI inhibitors through targeted medicinal chemistry approaches aimed at enhancing these critical contacts.

Table 1: The obtained docking features predicted by AutoDock program

Complex	***Synthase LasI / Genistein***	***Synthase LasI / Daidzein***	***Synthase LasI / Glycitein***
Cluster rank	1	1	1
Number in cluster	198	200	128
Lowest Binding Energy (kcal/mol)	-7.51	-7.90	-7.82
K_i(µM)	3.13	1.62	1.85

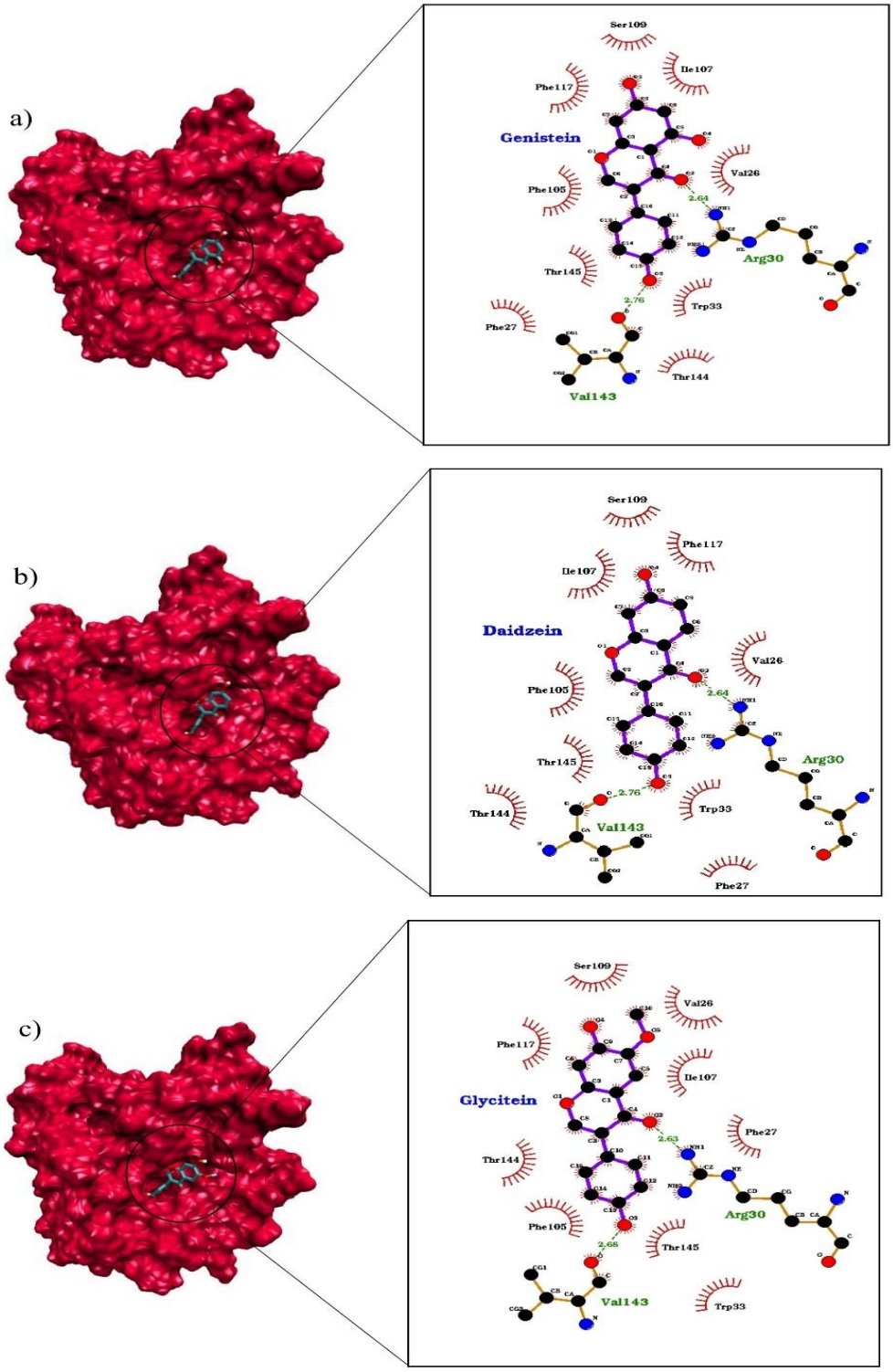

Fig. 1: Predicted docking modes and molecular interactions between Ligands and enzyme residues in the a) Synthase LasI/Genistein, b) Synthase LasI/Daidzein , and c) Synthase LasI/Glycitein systems using AutoDock software. The C, N, and O atoms are represented by black, blue, and red colors respectively. Figures generated using VMD1.9.3 and Ligplot^{+} programs

Molecular dynamic simulation

To corroborate and expand upon our molecular docking results, we conducted extensive 200 ns molecular dynamics (MD) simulations for the Synthase LasI enzyme in both its unbound state and complexed with each isoflavonoid ligand (genistein, daidzein, and glycitein). These simulations were essential to assess the stability of the complexes and monitor the temporal evolution of protein-ligand interactions under conditions mimicking the physiological environment. Our investigation centered on several critical metrics that offer insights into the system's behavior: 1) root mean square deviation (RMSD) to evaluate structural steadiness, 2) root mean square fluctuation (RMSF) to probe per-residue flexibility, 3) radius of gyration (Rg) to measure overall compactness, 4) solvent accessible surface area (SASA) to determine surface exposure changes, and 5) hydrogen bond formation patterns to characterize interaction persistence. Furthermore, we applied the molecular mechanics Poisson–Boltzmann surface area (MMPBSA) method to compute binding free energies and identify the principal thermodynamic components stabilizing the complexes.

RMSD analysis The RMSD analysis (Fig. 2) revealed distinct stabilization profiles for each Synthase LasI system, providing crucial insights into the differential effects of isoflavonoid binding on the enzyme's dynamic stability. A detailed examination of the trajectories shows significant variations in the time required for each system to reach equilibrium.

For the Synthase LasI/Genistein complex (Fig. 2a), a marked difference in equilibration kinetics was observed. The bound form reached a stable equilibrium significantly earlier, at approximately 120 ns, and maintained a consistently lower fluctuation profile throughout the simulation. In stark contrast, the apo form required a longer duration, stabilizing only at approximately 160 ns. This earlier equilibration and the complex's final lower mean RMSD of 0.169 ± 0.011 nm (compared to the apo's 0.202 ± 0.019 nm, Table 2) indicate that Genistein binding not only enhances the structural stability of the enzyme but also accelerates the convergence to a stable conformational state. This profile suggests Genistein acts primarily through a competitive inhibition mechanism. It likely binds directly to the enzyme's active site with high affinity, forming a stable complex that restricts essential conformational motions and prevents the native substrate from binding.

The Synthase LasI/Daidzein complex (Fig. 2b) exhibited a different behavior. In this case, both the apo and bound forms reached equilibrium at approximately the same time, around 160 ns. Post-equilibration, the bound form showed a marginally higher final mean RMSD (0.209 ± 0.030 nm) compared to the free enzyme (0.202 ± 0.019 nm). The increased average further suggests greater residual flexibility within the complex. This implies that while Daidzein binds with the highest affinity (as per docking results, Table 1), its binding mode does not hasten structural stabilization and may induce major conformational dynamics or flexibility in the enzyme structure. This dynamic profile is not typical of a classic competitive inhibitor. Instead, it suggests Daidzein may function through an allosteric mechanism

The Synthase LasI/Glycitein system (Fig. 2c) displayed the most pronounced effect on equilibration kinetics. The bound form reached equilibrium remarkably quickly, at approximately 80 ns, demonstrating a rapid and stable binding event. Meanwhile, the apo form required a full 160 ns to stabilize. This dramatically faster equilibration, coupled with a final mean RMSD (0.195 ± 0.022 nm) that is nearly identical to the apo form's (0.202 ± 0.019 nm), indicates that Glycitein binding induces minimal perturbation to the enzyme's global backbone structure while profoundly accelerating its transition to a stable conformational state. This suggests a highly complementary and stabilizing fit, con-

sistent with an efficient competitive inhibition mechanism.

These findings collectively illustrate the nuanced impact of each isoflavonoid on Synthase LasI's dynamics. Genistein and Glycitein significantly accelerate the enzyme's transition to a stable state while enhancing or maintaining structural rigidity, respectively. Daidzein highest binding affinity, may act as an allosteric inhibition, subtly altering the enzyme's dynamics with enhanced flexibility and disruption the functionality and structural integrity of the Synthase LasI.

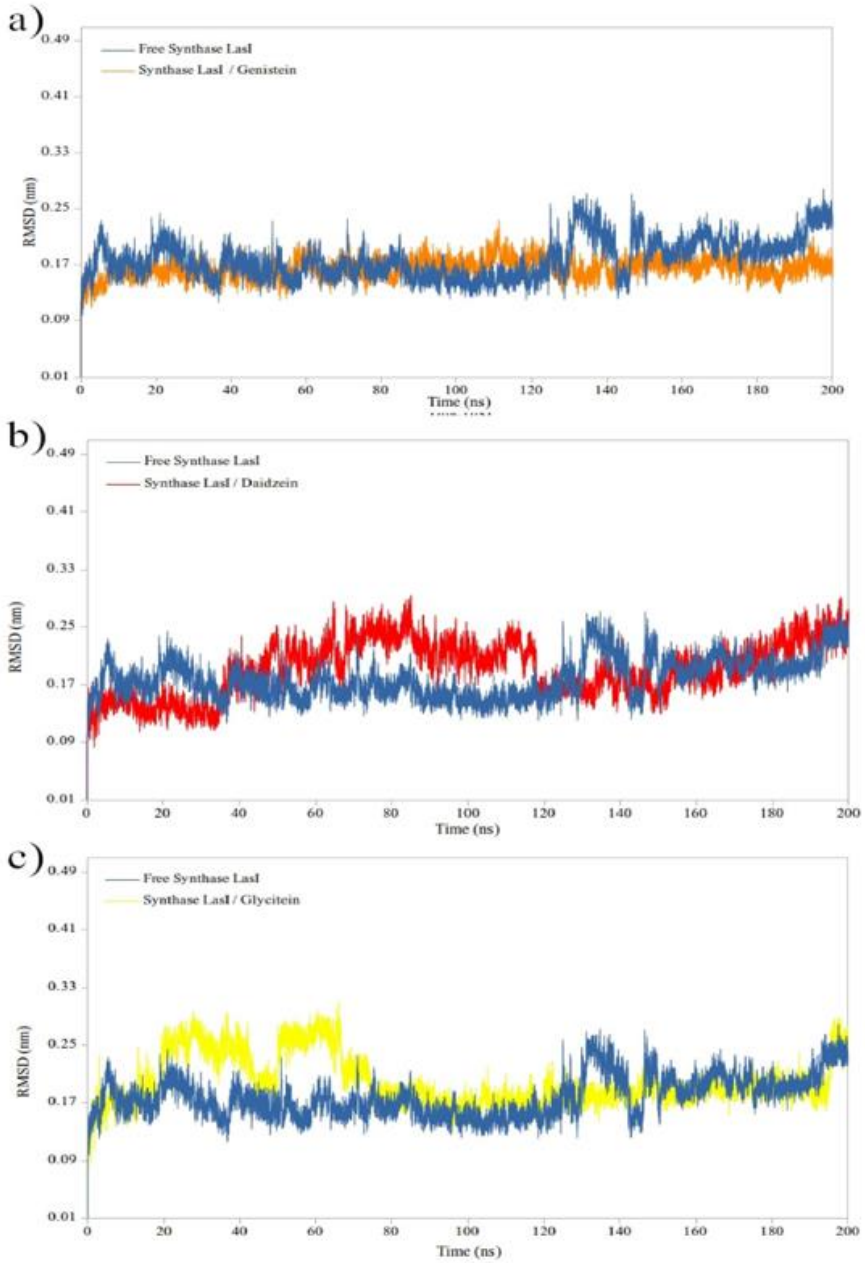

Fig. 2: RMSD plots of free and bound enzymes for a) Synthase LasI/Genistein, b) Synthase LasI/Daidzein , and c) Synthase LasI/Glycitein systems during the whole 200 ns simulation time

Table 2: The average and standard deviations of RMSD, Rg, RMSF and SASA for free and complex enzymes during the last 50ns

Complex	*Mean RMSD (nm)*	*Mean Rg (nm)*	*Mean RMSF (nm)*	*Mean SASA (nm^2)*
Free Synthase LasI	0.202 ± 0.019	1.626 ± 0.011	0.116 ± 0.051	103.952 ± 2.330
Synthase LasI/ Genistein	0.169 ± 0.011	1.629 ± 0.006	0.098 ± 0.052	104.46 ± 1.976
Synthase LasI/ Daidzein	0.209 ± 0.030	1.634 ± 0.009	0.124 ± 0.088	105.78 ± 2.347
Synthase LasI/ Glycitein	0.195 ± 0.022	1.615 ± 0.008	0.102 ± 0.051	102.79 ± 2.255

RG analysis

Complementing the RMSD findings, Rg measurements provided essential insights into the tertiary structural alterations induced by isoflavonoid binding in the Synthase LasI systems. The Rg parameter, which quantifies the spatial distribution of atomic mass relative to the protein's center of mass, serves as a sensitive indicator of global structural compaction or expansion. Analysis of the Rg trajectories (Fig. 3) revealed distinct ligand-specific structural responses that align closely with the RMSD profiles.

For the Synthase LasI/Genistein complex, Rg values exhibited minimal deviation upon ligand binding. The complexed form demonstrated a mean Rg of 1.629 ± 0.006 nm, nearly identical to the apo form (1.626 ± 0.011 nm) during the production phase (last 50 ns, Table 2). This consistency suggests that Genistein binding enhances structural stability without perturbing the overall tertiary architecture, supporting a binding mode that complements the native enzyme conformation.

In the Synthase LasI/Daidzein complex, a slight increase in Rg was observed, with the bound state measuring 1.634 ± 0.009 nm compared to 1.626 ± 0.011 nm for the unbound enzyme. This marginal expansion correlates with previously noted increases in structural flexibility (RMSD), indicating that Daidzein binding may induce a de compaction of the tertiary structure, potentially enhancing conformational dynamics.

Conversely, the Synthase LasI/Glycitein complex exhibited a pronounced compaction, with the bound form yielding an Rg of 1.615 ± 0.008 nm—significantly lower than that of the free enzyme (1.626 ± 0.011 nm). This reduction in Rg signifies enhanced global compactness and structural rigidity, consistent with the rapid equilibration and reduced fluctuations observed in RMSD analysis. This suggests that Glycitein binding promotes a more condensed and stable tertiary conformation. Temporal analysis of the Rg trajectory for Glycitein (Fig. 3c) indicates that this compaction is rapidly established and sustained throughout the simulation, aligning with its swift RMSD stabilization. This suggests an immediate and sustained effect on the enzyme's structural ensemble, leading to a more ordered and compact state.

Collectively, these Rg results elucidate the diverse structural impacts of isoflavonoid binding: Genistein preserves native compactness, Daidzein induces expansion, and Glycitein significantly enhances global compaction. These findings highlight the role of ligand-specific interactions in modulating the structural plasticity and thermodynamic stability of Synthase LasI, underpinning their potential as distinct mechanistic inhibitors.

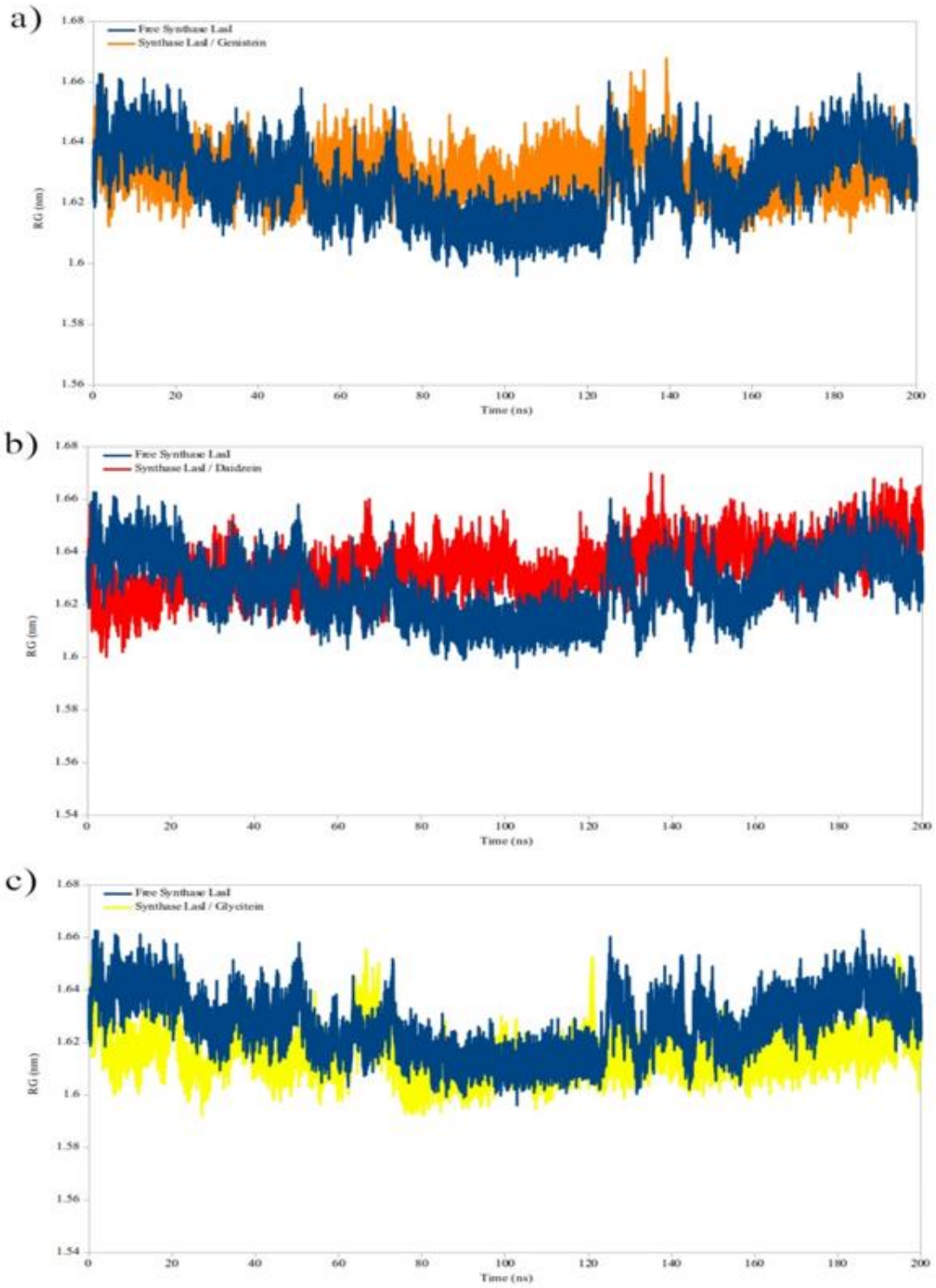

Fig. 3: Radius of gyration (Rg) plots of free and bound enzymes for a) Synthase LasI/Genistein, b) Synthase LasI/Daidzein , and c) Synthase LasI/Glycitein systems during the whole 200 ns simulation time

RMSF analysis

The RMSF results for Synthase LasI show that while the core structural elements of the enzyme remain relatively stable, specific loops and terminal regions display significant flexibility. In its free state, the enzyme exhibits the greatest movement in regions associated with binding and solvent interaction, a characteristic that makes biological sense for facilitating ligand binding and molecular recognition. In contrast, the putative catalytic and structural core regions remain quite rigid, which is essential for maintaining the enzyme's precise functional geometry.

Upon ligand binding, we see consistent but distinct reductions in flexibility across the three complexes, with the most noticeable effects occurring in key regions. The more distant N- and C-terminal regions of the enzymes largely retain their flexibility, showing that the ligands' effects are localized to the binding pocket and its adjacent loops rather than causing widespread changes to the entire enzyme structure. Together, these observations suggest that the isoflavonoids work by subtly limiting the natural movement of specific loops, potentially those involved in substrate recruitment or binding, rather than causing major structural rearrangements.

Looking at each complex individually, the Synthase LasI/Genistein complex (Fig. 4a) demonstrates the most pronounced stabilizing effect. This is quantified by its significantly lower mean RMSF value (0.098 ± 0.052 nm) compared to the free enzyme (0.116 ± 0.051 nm). Genistein binding results in a widespread suppression of fluctuations across multiple residue ranges, particularly in the regions between residues 20-80 and 100-170. This strong reduction in flexibility indicates that Genistein forms extensive interactions that effectively dampen the intrinsic dynamics of the enzyme, locking it into a more rigid and stable conformation.

The Synthase LasI/Daidzein complex (Fig. 4b) presents a contrasting profile. The bound system shows a marginally higher mean RMSF (0.124 ± 0.088 nm) than the free enzyme. The RMSF trajectory indicates that while some regions become slightly more stable, others, particularly around residues 20-40 and 80-100 and the C-terminal region, exhibit increased fluctuations. This suggests that Daidzein binding does not uniformly stabilize the structure but may induce a degree of dynamic flexibility or allosteric rearrangement in specific loops, correlating with its observed higher RMSD and Rg. The Synthase LasI/Glycitein complex (Fig. 4c) shows a focused and effective stabilization. The mean RMSF (0.102 ± 0.051 nm) is lower than that of the apo enzyme, indicating an overall reduction in flexibility.

Although the changes in flexibility vary in magnitude and nature, the fact that they consistently occur in specific regions suggests a common theme of targeted dynamic modulation. The isoflavonoids appear to function by selectively restricting the natural flexibility of loops that are crucial for enzyme function. By reducing these motions, the ligands likely impede the conformational changes necessary for substrate binding or catalysis, even though they do not dramatically alter the enzyme's overall fold. Genistein and Glycitein acts as a global stabilizer, and Daidzein may introduce specific flexibility that could be linked to an alternative inhibitory mechanism.

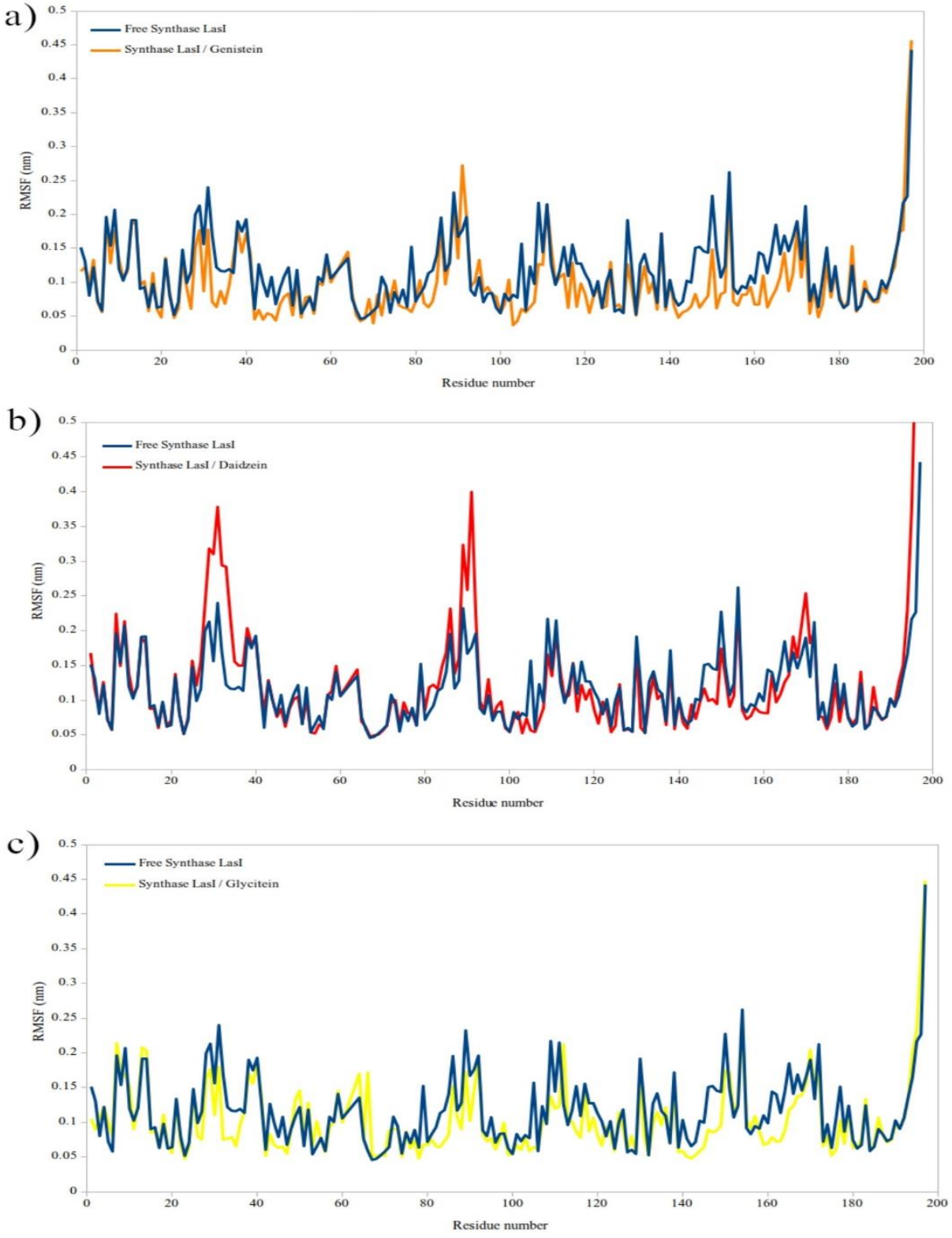

Fig. 4: RMSF plots of free and bound enzymes for a) Synthase LasI/Genistein, b) Synthase LasI/Daidzein , and c) Synthase LasI/Glycitein systems

SASA analysis

The analysis of the SASA trajectories (Fig. 5) and their averaged values (Table 2) provides a crucial dimension to our understanding of the structural dynamics induced by isoflavonoid binding, revealing how each ligand uniquely modulates the enzyme's interaction with its aqueous environment.

Fig. 5a (Synthase LasI/Genistein) shows a SASA trajectory for the complex that is remarkably congruent with the apo enzyme throughout the entire 200 ns simulation. Both systems reach a stable equilibrium by approximately 130 ns and maintain a consistent oscillation around nearly identical mean values. The plot visually confirms the quantitative data in Table 2, which shows a marginal, statistically insignificant increase in mean SASA for the complex (104.46 ± 1.976 nm²) compared to the apo form (103.952 ± 2.330 nm²). This indicates that Genistein binding achieves its potent stabilizing effect (as seen in low RMSD/RMSF) without perturbing the global solvation surface of the enzyme. This is characteristic of a ligand that binds with high complementarity, stabilizing the internal structure while perfectly preserving the external topological features of the native state.

Fig. 5b (Synthase LasI/Daidzein) presents a distinctly different profile. The trajectory for the complex consistently runs above that of the apo enzyme for the majority of the simulation time, particularly after the 50 ns mark. This visual expansion of the solvent-accessible surface is quantitatively confirmed by the highest mean SASA value of 105.78 ± 2.347 nm² (Table 2). This indicates a greater degree of dynamic flexibility in the bound state. This sustained increase in SASA provides direct visual evidence that Daidzein binding induces a loosening of the tertiary structure, exposing hydrophobic patches to the solvent. This mechanism aligns perfectly with its higher RMSD and Rg values, painting a coherent picture of a more dynamic and expanded complex.

Fig. 5c (Synthase LasI/Glycitein) reveals the most significant visual shift. The trajectory for the complex is clearly and consistently displaced below the apo enzyme's graph for the entire simulation duration after initial equilibration. This pronounced and sustained reduction in solvent-accessible surface is quantitatively robust, with the complex exhibiting the lowest mean SASA value of 102.79 ± 2.255 nm² (Table 2). The plot shows that this compaction is not a transient event but a stable property of the complex. This provides unambiguous evidence that Glycitein binding drives a global compaction of the enzyme structure. This forces a more efficient packing of the protein interior, burying hydrophobic residues and reducing the overall surface area exposed to the solvent. This observation is entirely consistent with Glycitein’s reduction in Rg and its strong, favorable van der Waals energy component (-169.341 ± 9.399 kJ/mol, Table 4), which is the primary driver of its binding. The SASA results complete our multidimensional assessment of Synthase LasI's structural response, showing how the same biological endpoint (enzyme inhibition) can be achieved through different biophysical pathways. This diversity in mechanism may prove advantageous for developing targeted therapies that inhibit Synthase LasI through complementary structural disruptions.

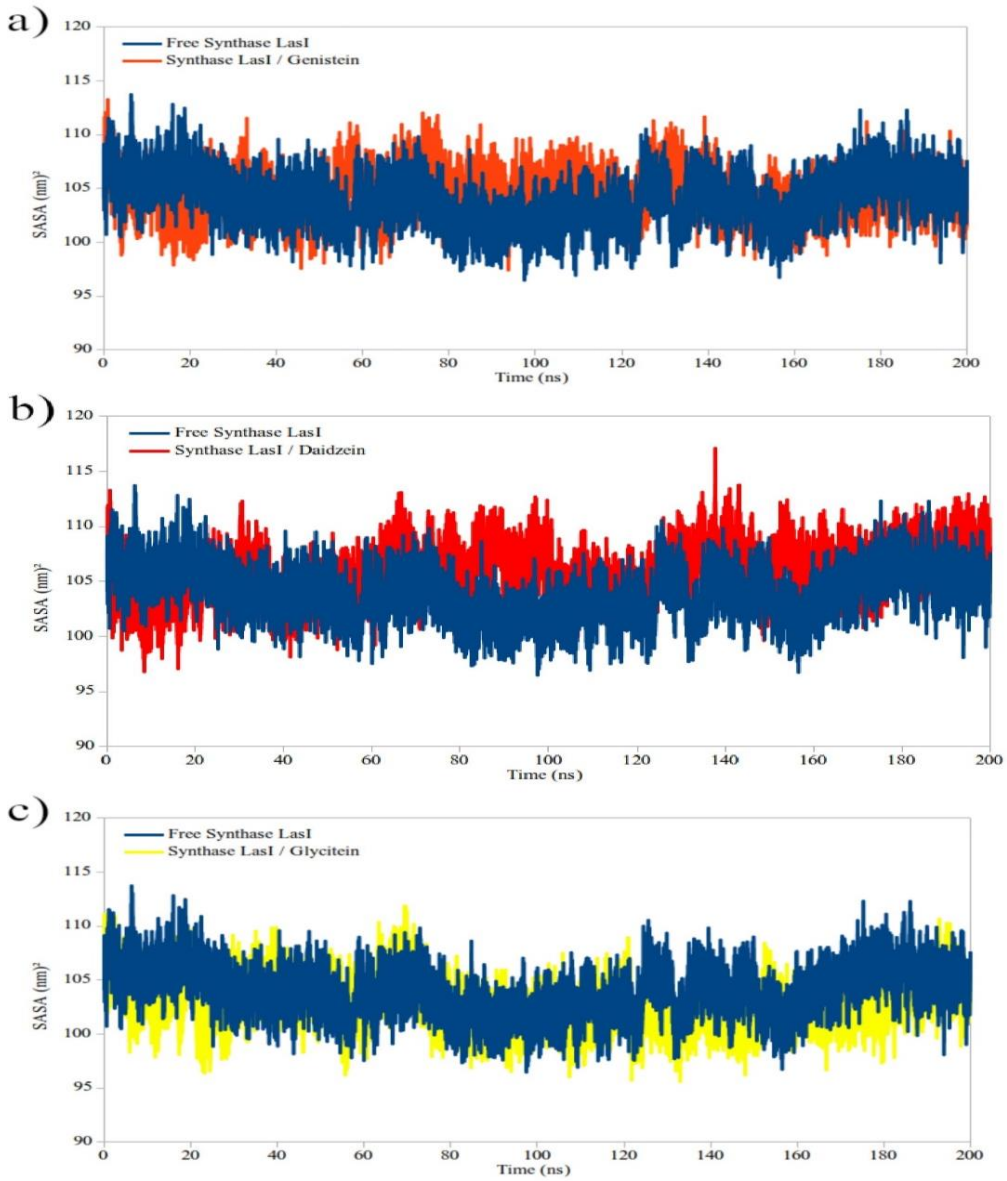

Fig. 5: SASA plots of free and bound enzymes for a) Synthase LasI/Genistein, b) Synthase LasI/Daidzein , and c) Synthase LasI/Glycitein systems during the whole 200 ns simulation time

Interactional analysis

The hydrogen bonding patterns and binding energetics provide critical insights into the molecular interactions stabilizing the Synthase LasI-ligand complexes, revealing distinct mechanistic profiles for each isoflavonoid.

Analysis of the hydrogen bond trajectories (Fig. 6) reveals how ligand binding differentially stabilizes the Synthase LasI system through distinct modifications of its interaction landscape. Throughout the 200 ns simulations, all three ligands formed stable hydrogen bonds with the enzyme. Synthase LasI/Genistein (Fig. 6a) maintained the consistent and extensive network, forming a stable with maximum of 5 hydrogen bonds throughout the simulation time. Synthase LasI/Daidzein (Fig. 6b) exhibited a more dynamic profile, forming maximum number of 6 hydrogen bonds with greater variability, suggesting a binding mode that allows for

more flexibility in its polar interactions. Synthase LasI/Glycitein (Fig. 6c) formed a stable but smaller network of 3 hydrogen bonds.

The profound effects of ligand binding are further evident when examining the propagation of these interactions through the enzyme's intramolecular and solvation networks (Fig. 7 and Fig. 8). For the Synthase LasI/Genistein complex, the binding event triggers a significant restructuring of the hydrogen bonding architecture. We observe a slight increase in intramolecular hydrogen bonds (158.912 ± 5.919) compared to the apo form (157.549 ± 5.811), accompanied by a substantial reduction in solvent hydrogen bonds (401.436 ± 12.620 vs 408.388 ± 12.939). This dual effect suggests Genistein binding induces a global structural tightening, where the formation of new internal hydrogen bonds and the ligand's own persistent H-bonds compensate for the displacement of water molecules from the binding site.

The Synthase LasI/Daidzein complex exhibits a different response. It shows a marginal decrease in intramolecular H-bonds (156.001 ± 6.208) and a smaller reduction in solvent H-bonds (406.731 ± 12.972) compared to the apo form. This pattern suggesting that its binding site remains somewhat accessible to water, leading to the greater overall flexibility we saw in the RMSD and Rg analyses. In contrast, the Synthase LasI/Glycitein complex presents a unique case. It shows a significant increase in intramolecular H-bonds (158.775 ± 6.023) alongside a pronounced reduction in solvent H-bonds (390.792 ± 12.112), the largest decrease among all complexes. This indicates that Glycitein binding promotes a dramatic restructuring of the hydrogen bonding network, favoring a more internally bonded, de solvated, and compact structure, which is entirely consistent with its lowest SASA and Rg values.

MMPBSA calculations

The MMPBSA calculations (Table 4) quantitatively affirm the stability trends inferred from hydrogen bonding and provide the thermodynamic rationale for the observed structural effects.

Synthase LasI/Genistein emerged as the strongest binder with a binding energy of -188.719 ± 8.675 kJ/mol. This superior affinity is overwhelmingly driven by exceptionally robust van der Waals contributions (-225.231 ± 8.983 kJ/mol), which constitute nearly the entirety of the favorable energy. The minimal electrostatic contribution (-2.906 ± 3.387 kJ/mol) and a moderate polar solvation penalty (52.231 ± 3.614 kJ/mol) indicate a binding mode dominated by shape complementarity and hydrophobic packing, perfectly explaining its strong stabilization without major structural perturbation.

Synthase LasI/Daidzein demonstrated significant but intermediate binding affinity (-118.179 ± 8.564 kJ/mol). Its binding is characterized by a strong van der Waals component (-154.077 ± 9.395 kJ/mol) and a notably more favorable electrostatic energy (-11.408 ± 4.899 kJ/mol) compared to the other ligands, suggesting a greater role for polar interactions. However, this is offset by a higher polar solvation penalty (61.480 ± 5.311 kJ/mol), which moderates its overall binding energy. This energetic profile aligns with its dynamic binding mode, allowing for strong but flexible interactions.

Synthase LasI/Glycitein, while having the least favorable net binding energy (-105.614 ± 10.421 kJ/mol), displays a strong van der Waals component (-169.341 ± 9.399 kJ/mol). Its binding is severely hampered by the largest polar solvation penalty (81.955 ± 8.071 kJ/mol), indicating a significant energetic cost to desolvating the ligand and the binding site. This explains its mechanism: the strong hydrophobic driving force is powerful enough to pay the cost for extensive de solvation and dramatic structural compaction, resulting in the tightly packed complex observed in the Rg and SASA analyses

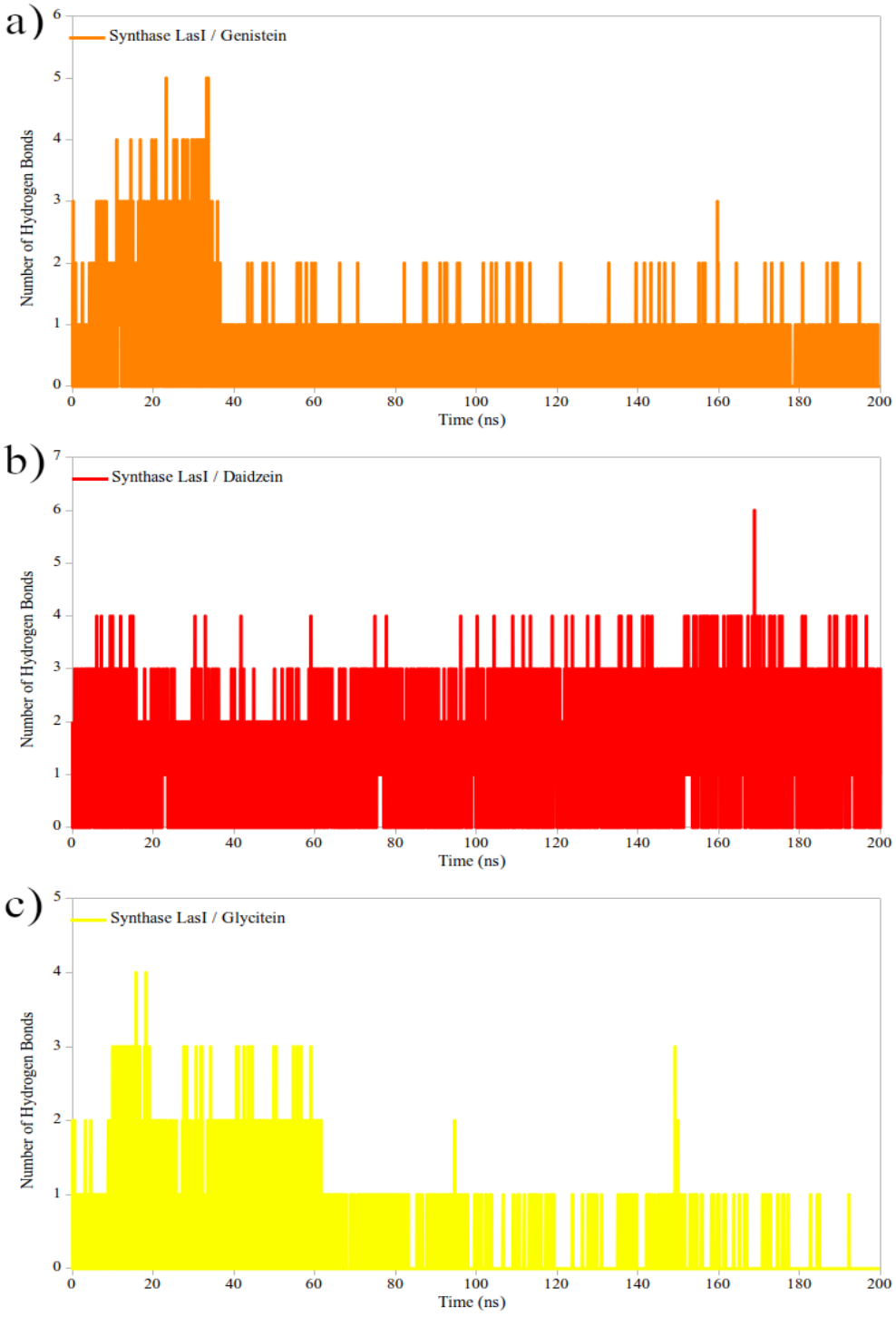

Fig. 6: Time dependence of the number of hydrogen bonds between Curcumin and enzymes for a) Synthase LasI/Genistein, b) Synthase LasI/Daidzein , and c) Synthase LasI/Glycitein systems during the simulation time

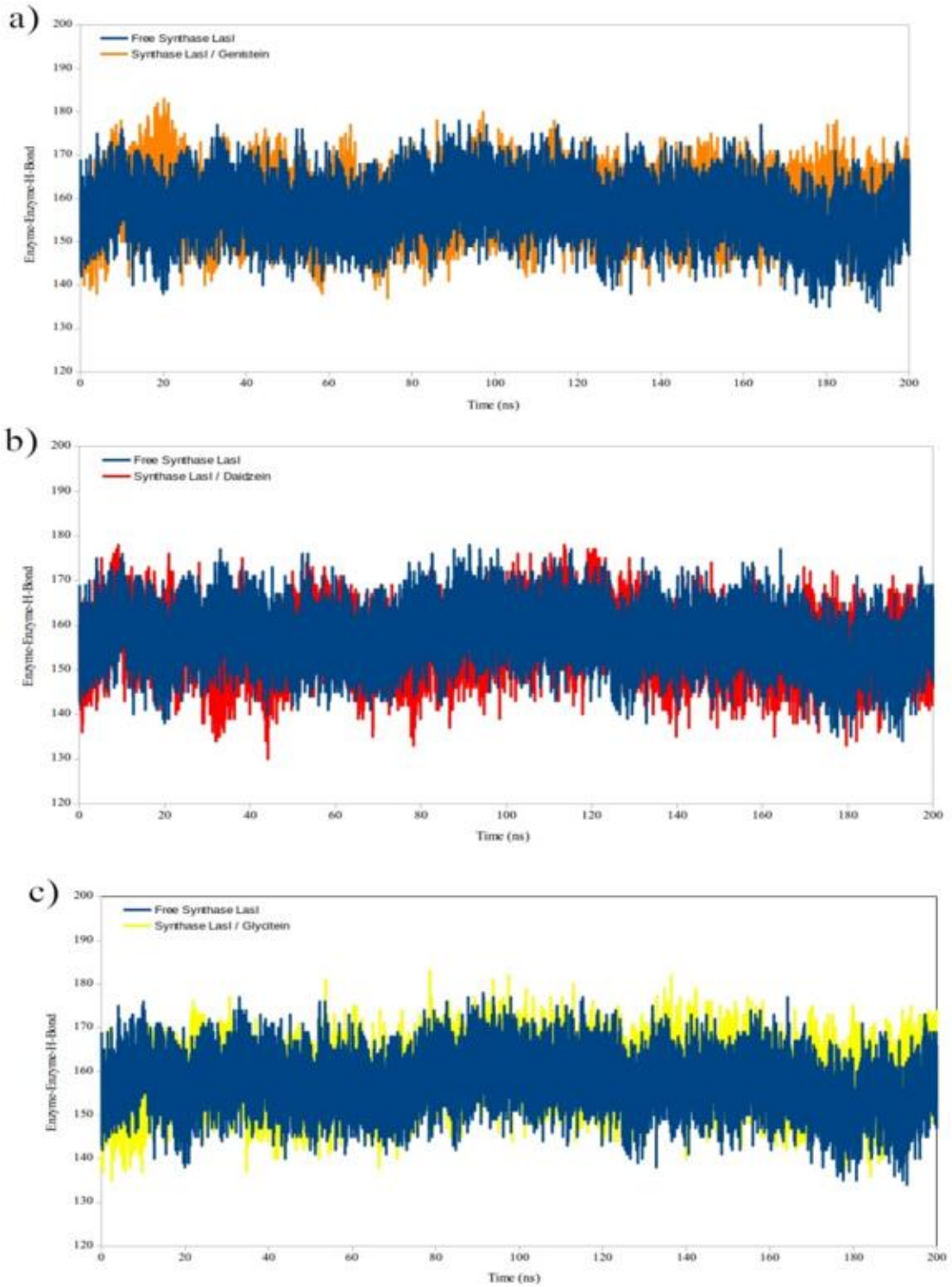

Fig. 7: Intramolecular enzyme hydrogen-bond plots of free and bound enzymes for a) Synthase LasI/Genistein, b) Synthase LasI/Daidzein , and c) Synthase LasI/Glycitein systems during the whole 200 ns simulation time

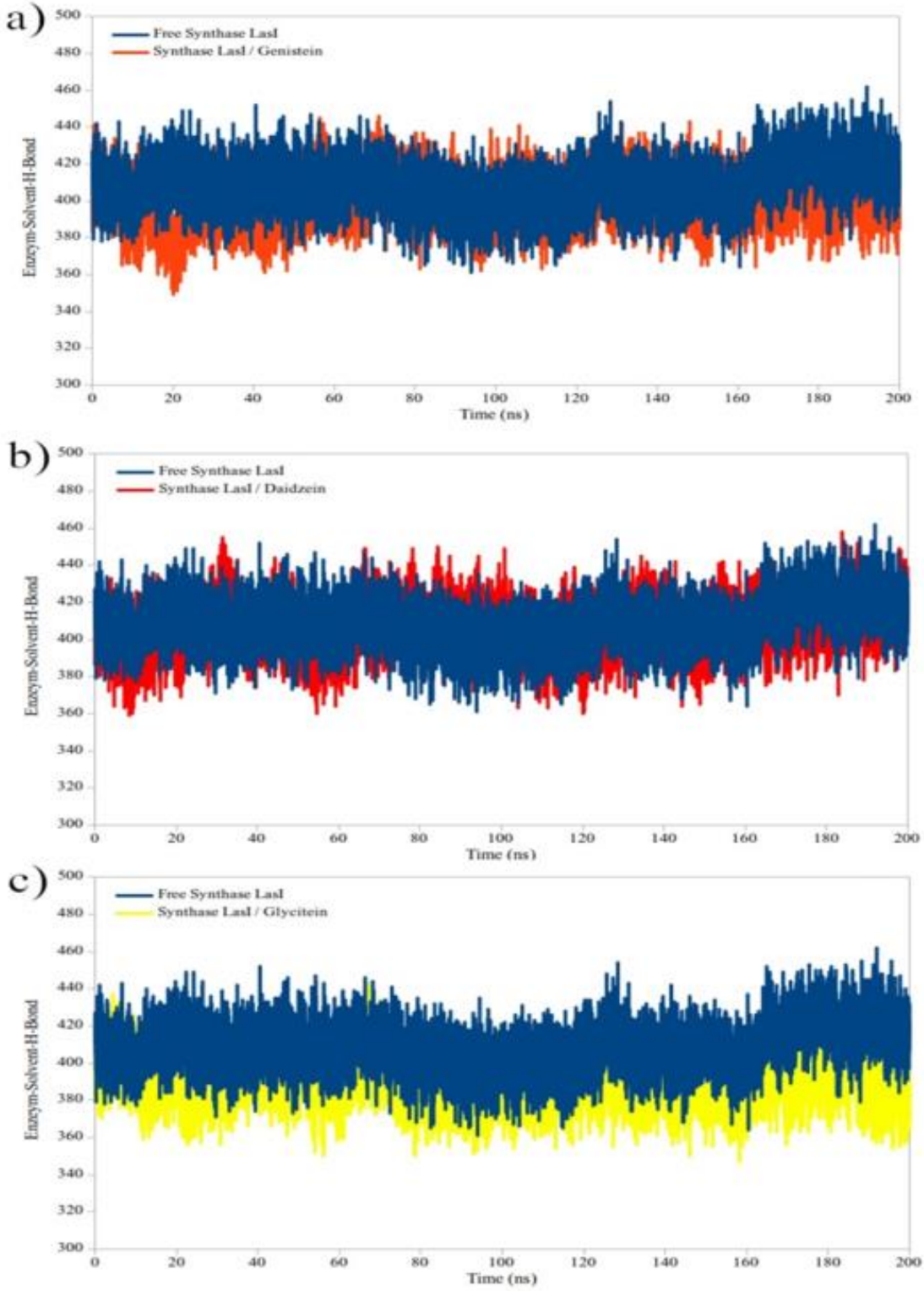

Fig. 8: Enzyme–solvent hydrogen-bond plots of free and bound enzymes for a) Synthase LasI/Genistein, b) Synthase LasI/Daidzein , and c) Synthase LasI/Glycitein systems during the whole 200 ns simulation time

Table 3: The average and standard deviations of intra molecular enzyme and enzyme-solvent hydrogen bonds during last 50 ns

System	*Enzyme-Enzyme*	*Enzyme-Solvent*
Free Synthase LasI	157.549 ± 5.811	408.388 ± 12.939
Synthase LasI/ Genistein	158.912 ± 5.919	401.436 ± 12.620
Synthase LasI/ Daidzein	156.001 ± 6.208	406.731 ± 12.972
Synthase LasI/ Glycitein	158.775 ± 6.023	390.792 ± 12.112

Table 4: The average of energy components for complexes analyzed by MMPBSA

Energy components (kJ/mol)	*Synthase LasI / Genistein*	*Synthase LasI / Daidzein*	*Synthase LasI / Glycitein*
van der Waal energy	-225.231+/-8.983	-154.077+/-9.395	-169.341+/-9.399
Electrostatic energy	-2.906+/-3.387	-11.408+/-4.899	-2.683+/-3.678
Polar solvation energy	52.231+/-3.614	61.480+/-5.311	81.955+/-8.071
SASA energy	-12.813+/-0.633	-14.174+/-0.706	-15.546+/-0.772
Binding energy	-188.719+/-8.675	-118.179+/-8.564	-105.614+/-10.421

Discussion

This computational study reveals that soy isoflavonoids, particularly genistein, daidzein, and glycitein, exhibit distinct inhibitory profiles against the *P. aeruginosa* QS synthase LasI. The binding of these compounds, especially to residues Arg30 and Val143, and their subsequent effects on enzyme stability and dynamics, contribute valuable insights into flavonoid-based anti-virulence strategies.

When compared to recent literature, these findings find strong validation, intriguing contrasts, and open new avenues for the rational design of QS inhibitors. Our molecular docking analysis, which identified Arg30 and Val143 as critical for isoflavonoid binding, is strongly corroborated by mechanistic studies on synthetic inhibitors. Research on the thiazolidinedione derivative TZD-C8, a potent LasI inhibitor, utilized in silico docking and site-directed mutagenesis to conclusively demonstrate that residues Arg30 and Ile107 are essential for its inhibitory activity (45, 46). The abolition of TZD-C8's effect in a LasI double mutant (R30D, I107S) provides robust experimental validation for targeting this region of the enzyme's active site. This parallel underscores the reliability of our computational approach in predicting functionally relevant interactions and highlights Arg30 as a conserved hotspot for inhibitor design, whether the scaffolds are synthetic or natural.

While our study and the work on TZD-C8 focus on direct competitive binding to the synthase's active site, other research illustrates the diverse mechanisms by which natural products can disrupt QS circuitry. A study on the natural chalcone isoliquiritigenin demonstrated potent anti-virulence effects against *P. aeruginosa*, including the reduction of biofilm formation and virulence factor production (47). Interestingly, isoliquiritigenin was shown to downregulate the expression of key QS genes, including lasI, as measured by promoter-reporter assays (47). This suggests an upstream, transcriptional-level mechanism distinct from the direct enzyme inhibition proposed for our isoflavonoids. This comparison is instructive: it shows that effective QS inhibition can be achieved either by blocking the synthase's function (as with genistein) or by suppressing its production (as

with isoliquiritigenin), offering multiple strategic entry points for drug development.

Our molecular dynamics simulations suggested that daidzein may induce a degree of conformational flexibility in LasI, hinting at a potential allosteric or dynamic mode of inhibition. This concept is supported by pioneering work on the related synthase RhlI. Research on acyl-homoserine lactone (AHL) analogs targeting RhlI revealed the existence of two distinct binding pockets one for inhibitors and another for activators within the enzyme (48, 49). This discovery of allosteric sites in a LuxI-type synthase provides a plausible structural basis for the dynamic effects we observed with daidzein. It raises the compelling hypothesis that certain isoflavonoids might not only compete at the active site but also bind to secondary, regulatory pockets to modulate enzyme activity, a possibility meriting further investigation. The ultimate goal of anti-virulence strategies is to attenuate infection without promoting resistance. Both our findings and the broader literature affirm this promise. For instance, isoliquiritigenin was reported to develop no resistance over 20 generations and, crucially, to increase the sensitivity of P. aeruginosa to aminoglycoside antibiotics like tobramycin and amikacin (47, 50). This aligns perfectly with the strategic rationale for QS inhibition: by disarming the bacteria's virulence apparatus, these compounds can render pathogens more susceptible to host immune clearance and enhance the efficacy of conventional antibiotics, creating a powerful synergistic therapeutic approach.

Conclusion

Natural isoflavonoids, particularly genistein, can effectively target and stabilize the quorum-sensing synthase LasI in *P. aeruginosa*. Through integrated docking and dynamics simulations, we elucidated three distinct mechanistic classes: genistein as a stabilizer, daidzein as a de stabilizer, and glycitein as a compactor. The superior and stable binding of genistein, driven by potent van der Waals interactions, positions it as an ideal scaffold for rational inhibitor design. While this work provides high-resolution mechanistic insights, it remains a predictive model. Future work must include *in vitro* enzymatic assays to confirm inhibition potency (IC_{50}), structural studies (X-ray crystallography) to validate the binding pose, and *in vivo* models to assess efficacy in disrupting biofilm formation. Ultimately, targeting synthase LasI with optimized genistein derivatives presents a promising, narrow-spectrum strategy to combat *pseudomonas* infections by mitigating virulence without imparting selective pressure for resistance. This study is limited by its reliance on computational methods, which provide predictive rather than definitive evidence of inhibition. Docking and MD simulations cannot fully capture enzymatic kinetics or cellular context. Therefore, in vitro enzymatic assays, structural studies, and in vivo biofilm models are required to validate these findings.

Competing interests

The authors declare that they have no competing interests.

Acknowledgments

This research was supported by resources supplied by the deputy of financial affairs of the Ghalib University, Kabul, Afghanistan.

The authors would like to express their utmost gratitude to the Board of Directors of Ghalib University, Kabul, Afghanistan for support and motivations, especially Dr. M. I. Noori and Eng. A. Ahadi. Special thanks to Mr. Mohammad Yousoof Saleh (Head of HR and financial affairs of Ghalib University) and his team, for assisting us in better performance of this study.

References

1. Coque TM, Cantón R, Pérez-Cobas AE, Fernández-de-Bobadilla MD, Baquero F. Antimicrobial resistance in the global health network: known unknowns and challenges for efficient responses in the 21st century. Microorganisms. 2023;11(4):1050.
2. Bhagirath AY, Li Y, Somayajula D, Dadashi M, Badr S, Duan K. Cystic fibrosis lung environment and *Pseudomonas aeruginosa* infection. BMC Pulm Med. 2016;16(1):174.
3. Jaafar F, Bashar N, Alhusseini L, Musafer H. Infections with *Pseudomonas aeruginosa* in Burn Patients: The Host Immune Response. SARJBAB. 2023;5:15-21.
4. Panda SS, Singh K, Pati S, Singh R, Kant R, Dwivedi GR. Pseudomonas aeruginosa: pathogenic adapter bacteria. Antimicrobial Resistance: Underlying Mechanisms and Therapeutic Approaches: Springer; 2022. p. 113-35.
5. Mulcahy LR, Isabella VM, Lewis K. *Pseudomonas aeruginosa* biofilms in disease. Microb Ecol. 2014;68(1):1-12.
6. Bakke R, Trulear M, Robinson J, Characklis W. Activity of *Pseudomonas aeruginosa* in biofilms: steady state. Biotechnol Bioeng. 1984;26(12):1418-24.
7. Wang X, Liu M, Yu C, Li J, Zhou X. Biofilm formation: mechanistic insights and therapeutic targets. Mol Biomed. 2023;4(1):49.
8. Stewart P, Bjarnsholt T. Risk factors for chronic biofilm-related infection associated with implanted medical devices. Clin Microbiol Infect. 2020;26(8):1034-8.
9. Ray RR, Nag M, Lahiri D. Biofilm-mediated diseases: causes and controls: Springer; 2021.
10. Xu Q, Hu X, Wang Y. Alternatives to conventional antibiotic therapy: potential therapeutic strategies of combating antimicrobial-resistance and biofilm-related infections. Mol Biotechnol. 2021;63(12):1103-24.
11. Gebreyohannes G, Nyerere A, Bii C, Sbhatu DB. Challenges of intervention, treatment, and antibiotic resistance of biofilm-forming microorganisms. Heliyon. 2019;5(8).
12. Kalia VC. Quorum sensing inhibitors: an overview. Biotechnol Adv. 2013;31(2):224-45.
13. Moreno-Gámez S, Hochberg ME, Van Doorn G. Quorum sensing as a mechanism to harness the wisdom of the crowds. Nat Commun. 2023;14(1):3415.
14. Srikanth P, Sivakumar D, Nouri J. Environmental microbial communications in gram-positive and gram-negative bacteria. Glob J Environ Sci Manag. 2023;9:1-20.
15. Kostylev M, Kim DY, Smalley NE, Salukhe I, Greenberg EP, Dandekar AA. Evolution of the *Pseudomonas aeruginosa* quorum-sensing hierarchy. Proc Natl Acad Sci U.S.A. 2019;116(14):7027-32.
16. Papenfort K, Bassler BL. Quorum sensing signal–response systems in Gram-negative bacteria. Nat Rev Microbiol. 2016;14(9):576-88.
17. Stevens AM, Queneau Y, Soulere L, Bodman Sv, Doutheau A. Mechanisms and synthetic modulators of AHL-dependent gene regulation. Chem Rev. 2011;111(1):4-27.
18. Rodríguez-Urretavizcaya B, Vilaplana L, Marco M-P. Strategies for quorum sensing inhibition as a tool for controlling *Pseudomonas aeruginosa* infections. Int J Antimicrob Agents. 2024;64(5):107323.
19. Statsenko ES, Shtarberg MA, Borodin EA. Isoflavonoids in soy and soy-containing foods. 2022. https://www.semanticscholar.org/paper/Isoflavonoids-in-Soy-and-Soy-Containing-Foods-Statsenko-Shtarberg/6b2b6555516c7fc72d27155ab871856789b8d69a
20. Dhaubhadel S, McGarvey BD, Williams R, Gijzen M. Isoflavonoid biosynthesis and accumulation in developing soybean seeds. Plant Mol Biol. 2003;53(6):733-43.
21. Nakamura Y, Kaihara A, Yoshii K, Tsumura Y, Ishimitsu S, Tonogai Y. Content and composition of isoflavonoids in mature or immature beans and bean sprouts consumed in Japan. J Health Sci. 2001;47(4):394-406.
22. Mazumder MAR, Hongsprabhas P. Genistein as antioxidant and antibrowning agents in in vivo and in vitro: A review. Biomed Pharmacother. 2016;82:379-92.
23. Naeem H, Momal U, Imran M, Shahbaz M, Hussain M, Alsagaby SA, et al. Anticancer

perspectives of genistein: a comprehensive review. Int J Food Prop. 2023;26(2):3305-41.
24. Saha S, Sadhukhan P, C Sil P. Genistein: a phytoestrogen with multifaceted therapeutic properties. Int J Food Prop. 2014;14(11):920-40.
25. Evans M, Elliott JG, Sharma P, Berman R, Guthrie N. The effect of synthetic genistein on menopause symptom management in healthy postmenopausal women: a multi-center, randomized, placebo-controlled study. Maturitas. 2011;68(2):189-96.
26. Wang J, Shang F, Liu L, Wang J, Mei Q. In vivo and in vitro activity of genistein in osteoporosis. Indian J Pharm Pharmacol. 2007;39(2):103-6.
27. Pavese JM, Farmer RL, Bergan RC. Inhibition of cancer cell invasion and metastasis by genistein. Cancer Metastasis Rev. 2010;29(3):465-82.
28. Shafiee G, Saidijam M, Tayebinia H, Khodadadi I. Beneficial effects of genistein in suppression of proliferation, inhibition of metastasis, and induction of apoptosis in PC3 prostate cancer cells. Arch Physiol Biochem. 2022;128(3):694-702.
29. Akhlaghipour I, Nasimi Shad A, Askari VR, Baradaran Rahimi V. Daidzin and its de-glycosylated constituent daidzein as a potential therapeutic for cardiovascular diseases: A review from bench to bed. Phytother Res. 2024;38(8):3973-85.
30. Tekin I, Gundogdu G, Kilic-Erkek O, Buber I, Akca H, Yaylali YT, et al. Cardioprotective effects of daidzein: Exploring the role of the NRG-1/Akt pathway in a rat model of isoproterenol-induced myocardial infarction. NMCD. 2025:104204.
31. Rafii F. The role of colonic bacteria in the metabolism of the natural isoflavone daidzin to equol. Metabolites. 2015;5(1):56-73.
32. Stephens BR, Bomser JA. Glycitein in health. 2012. Doi: https://doi.org/10.1039/9781849735094-00465
33. Song TT, Hendrich S, Murphy PA. Estrogenic activity of glycitein, a soy isoflavone. J Agric Food Chem. 1999;47(4):1607-10.
34. Dong N, Yang Z. Glycitein exerts neuroprotective effects in Rotenone-triggered oxidative stress and apoptotic cell death in the cellular model of Parkinson's disease. Acta Biochim Pol. 2022;69(2):447-52.
35. Luo X, Wang Z, Xu J, Gao Z, Song Z, Wang W. Hemoglobin binding and antioxidant activity in spinal cord neurons: O-methylated isoflavone glycitein as a potential small molecule. Acta Biochim Pol. 2023;16(10):105164.
36. Patel DK. Therapeutic potential of a bioactive flavonoids glycitin from Glycine max: a review on medicinal importance, pharmacological activities and analytical aspects. Curr Tradit Med. 2023;9(2):33-42.
37. Makarewicz M, Drożdż I, Tarko T, Chodak A. The interactions between polyphenols and microorganisms, especially gut microbiota. Antioxidants 2021, 10, 188. GUT microbiota, SCFA. 2021:157.
38. De Rossi L, Rocchetti G, Lucini L, Rebecchi A. Antimicrobial potential of polyphenols: Mechanisms of action and microbial responses—A narrative review. Antioxidants. 2025;14(2):200.
39. Chaubey S, Mishra V, Verma M, Ashraf Som. Phytochemicals as Antimicrobial Agent to Combat AntibioticResistance in Microbial Pathogens.
a. https://www.academia.edu/download/121187817/Manuscript_micro.pdf
40. Berman HM, Westbrook J, Feng Z, Gilliland G, Bhat TN, Weissig H, Shindyalov IN, Bourne PE. The Protein Data Bank. Nucleic Acids Res. 2000;28(1):235-42.
41. Sterling T, Irwin JJ. ZINC 15–ligand discovery for everyone. J Chem Inf Model. 2015;55(11):2324-37.
42. Chen Y, Shoichet BK. Molecular docking and ligand specificity in fragment-based inhibitor discovery. Nat Chem Biol. 2009;5(5):358-64.
43. Sousa da Silva AW, Vranken WF. ACPYPE-Antechamber python parser interface. BMC Res Notes. 2012;5:1-8.
44. Van Der Spoel D, Lindahl E, Hess B, Groenhof G, Mark AE, Berendsen HJ. GROMACS: fast, flexible, and free. J Comput Chem. 2005;26(16):1701-18.
45. Shin D, Gorgulla C, Boursier ME, Rexrode N, Brown EC, Arthanari H, et al. N-acyl homoserine lactone analog modulators of the *Pseudomonas aeruginosa* Rhll quorum sensing signal synthase. ACS Chem Biol. 2019;14(10):2305-14.

46. Lidor O, Al-Quntar A, Pesci E, Steinberg D. Mechanistic analysis of a synthetic inhibitor of the *Pseudomonas aeruginosa* LasI quorum-sensing signal synthase. Sci Rep. 2015;5(1):16569.
47. Song W, Tian Z, Wang Y, Yin Y, Zhang H, Xu C, et al. Isoliquiritigenin targets las, rhl, and Pqs quorum sensing systems to mitigate the virulence and infection of Pseudomonas aeruginosa. BMC Microbiol. 2025;25(1):580.
48. Maiga A, Ampomah-Wireko M, Li H, Fan Z, Lin Z, Zhen H, et al. Multidrug-resistant bacteria quorum-sensing inhibitors: A particular focus on Pseudomonas aeruginosa. Eur J Med Chem. 2025;281:117008.
49. Nazari MJ, Anwary MT, Ghazanfar K, Amiri ME, Hafid SY, Jawad MJ, et al. Inhibition of acyl-homoserine-lactone synthase in *Pseudomonas aeruginosa* biofilms by 7-O-methyl-aromadendrin by using molecular docking and molecular dynamics simulation. In Silico Pharmacol. 2025;13(1):1-16.
50. Alum EU, Gulumbe BH, Izah SC, Uti DE, Aja PM, Igwenyi IO, et al. Natural product-based inhibitors of quorum sensing: A novel approach to combat antibiotic resistance. Biochem Biophys Rep. 2025;43:102111.